TRAJECTORY OPTIMIZATION FOR THE NATIONAL AEROSPACE PLANE

FINAL REPORT

(June 13, 1992–October 30, 1993)

November, 1993

Research Supported by

NASA Langley Research Center

NASA Grant NO. NAG-1-1255

Technical Monitor: Dr. Daniel D. Moerder

Principal Investigator: Ping Lu

Department of Aerospace Engineering and Engineering Mechanics

Iowa State University

Ames, IA 50011

ACKNOWLEDGEMENTS

The support of NASA Langley Research Center under grant NAG-1-1255 and Dr. Daniel D. Moerder of Guidance and Control Division, Spacecraft Control Branch, who served as the technical monitor, are gratefully acknowledged.

TABLE OF CONTENTS

LIST OF SYMBOLS

C_D	Drag coefficient
C_L	Lift coefficient
C_T	Thrust coefficient
c	Command altitude
D	Aerodynamic drag
g_o	Gravitational acceleration (9.81 m/sec)
I_{sp}	Specific impulse
L	Aerodynamic lift
m	Mass (kg)
Q	Convective heating rate
Q_{max}	Maximum allowable level of Q
q	Dynamic pressure
q_{max}	Maximum allowable level of q
R_o	Radius of the Earth (6378 km)
r	Radius from the center of the Earth to the vehicle
T	Thrust
t	Time
v	Velocity
α	Angle of attack
ε	Thrust angle
ϕ	Latitude
γ	Flight path angle
ψ	Heading angle
μ	Gravitational parameter

σ	Bank angle
θ	Longitude
Ω	Fuel-equivalence ratio
superscript '	Derivative with respect to θ
subscript f	Final point

LIST OF FIGURES

1. Summary

This is a second phase research following the first phase which was from May 1, 1991 to May 30, 1992. The objective is to investigate the optimal ascent trajectory for the National AeroSpace Plane (NASP) from runway take-off to orbital insertion and address the unique problems associated with the hypersonic flight trajectory optimization. The trajectory optimization problem for an aerospace plane is a highly challenging problem because of the complexity involved. Previous work has been successful in obtaining suboptimal trajectories by using energy-state approximation and time-scale decomposition techniques [1–3]. But it is known that the energy-state approximation is not valid in certain portions of the trajectory. This research aims at employing full dynamics of the aerospace plane and emphasizing direct trajectory optimization methods.

The major accomplishments of this research include the first-time development of an inverse dynamics approach in trajectory optimization which enables us to generate optimal trajectories for the aerospace plane efficiently and reliably, and general analytical solutions to constrained hypersonic trajectories that has wide application in trajectory optimization as well as in guidance and flight dynamics. Optimal trajectories in abort landing and ascent augmented with rocket propulsion and thrust vectoring control were also investigated. Motivated by this study, a new global trajectory optimization tool using continuous simulated annealing and a nonlinear predictive feedback guidance law have been under investigation and some promising results have been obtained, which may well lead more significant development and application in the near future.

There have been a total of seven publications that were either supported or partially supported by this grant [4–10], and one has been submitted recently [11]. As a direct result of the support under this grant, a graduate student, John Samsundar, has received his Master Degree in Aerospace Engineering in 1993 [7]. Because these publications contain detailed descriptions of a large portion of the work, this report will only give brief summaries to those results that have been reported in the open literature. More detailed discussions are

provided for other findings that are not in the above cited publications.

2. Vehicle Model

The aerospace plane model used throughout this study is based on a winged-cone configuration developed at NASA Langley Research Center [12]. The aerodynamic coefficients are given in tabulated form as functions of angle of attack ranging from $-1°$ to $12°$, control surface deflections and Mach number ranging from 0.3 to 24.2. The thrust of the airbreathing propulsion system is proportional to dynamic pressure

$$T = C_T q$$

where the thrust coefficient C_T, as well as the specific impulse I_{sp}, depends on fuel equivalence ratio, dynamic pressure and Mach number, determined from table lookup. The vehicle has a weight of 300,000 lb and an overall fuselage length of 200 ft. This model has also been used in several other studies [13]. It is felt that the use of this model in the trajectory optimization problem has preserved essential characteristics of hypersonic vehicles which may otherwise not be prominent in other over-simplified models.

The three-dimensional point-mass motion of the aerospace plane over a spherical, non-rotating earth is described by

$$r' = \frac{r \tan\gamma \cos\phi}{\cos\psi} \tag{1}$$

$$\phi' = \tan\gamma \cos\phi \tag{2}$$

$$v' = \left(\frac{T\cos(\alpha-\varepsilon) - D}{M} - \frac{\mu \sin\gamma}{r^2}\right)\frac{r\cos\phi}{v\cos\gamma\cos\psi} \tag{3}$$

$$\gamma' = \left(\frac{(T\sin(\alpha-\varepsilon)+L)\cos\sigma}{mv} - \left(\frac{\mu}{vr^2} - \frac{v}{r}\right)\cos\gamma\right)\frac{r\cos\phi}{v\cos\gamma\cos\psi} \tag{4}$$

$$\psi' = \left(\frac{(T\sin(\alpha-\varepsilon)+L)\sin\sigma}{mv\cos\gamma} - \frac{v\cos\gamma\cos\psi\tan\phi}{r}\right)\frac{r\cos\phi}{v\cos\gamma\cos\psi} \tag{5}$$

$$m' = \frac{-T}{g_o I_{sp}}\frac{r\cos\phi}{v\cos\gamma\cos\psi} \tag{6}$$

where the prime ' indicates differentiation with respect to longitude θ. The use of θ as the independent variable is for convenience of the inverse dynamics approach described later.

3. Minimum-Fuel Ascent: Inverse Dynamics Approach

3.1 Two-Dimensional Ascent

In this problem, an optimal trajectory is sought for the aerospace plane from horizontal take-off to insertion into a circular orbit at a given altitude with minimum fuel consumption. In addition to the final orbit insertion conditions, two important flight path constraints are also necessary [14]

$$q \leq q_{max} \tag{7}$$

$$Q \leq Q_{max} \tag{8}$$

From an optimal control viewpoint this problem is very challenging due to several reasons: hypersonic trajectories are extremely sensitive to to variations in aerodynamic and propulsive forces, which renders the optimization problem to be poor-conditioned; the two functional constraints (7) and (8) only add significantly more difficulty to the already complex problems; the nonanalytical modeling of the vehicle makes any techniques based on calculus of variations inapplicable. To cope with these challenges, an inverse dynamics approach was developed. The idea is to specify a history of altitude profile, then solve for the controls required to fly this altitude history. By iteratively searching for the optimal ascent altitude history, the optimal controls are finally found. This approach, its advantages and extensive numerical results are given in [5], [8] and [14]. Reference [5] also discusses the use of the inverse dynamics approach in guidance for the aerospace plane. This technique was first tried on 2-D optimal ascent in which the controls are α and Ω, angle of attack and fuel equivalence ratio, respectively (ε is assumed to be zero). Figure 1 shows a typical optimal trajectory.

3.2 Three-Dimensional Ascent

The actual flight of the aerospace plane will not likely be restricted to 2-D flight, since some out-of-plane maneuvers may be required for given conditions at take-off and orbital

insertion. It would be of great interest to understand how the out-of-plane maneuvers will influence the fuel consumption along the minimum-fuel trajectory, and whether or not the conclusions from the study of 2-D flight will be valid for 3-D cases. While there is no more theoretical difficulty in 3-D flight than in 2-D case, the numerical difficulty is increased considerably because not only the number of state variables and controls in 3-D flight is increased, but also the inequality constraints (7) and (8) on the trajectory are more difficult to satisfy. With the confidence gained in the 2-D study with the inverse dynamics approach, it appears logical to continue to use this technique in 3-D problem. Now consider the equations of motion Eqs. (1)–(6). Let $c(\theta)$ be a specified profile of the radius

$$r(\theta) = c(\theta) \tag{9}$$

Differentiating Eq. (9) twice gives

$$\begin{aligned} \gamma' &= \cos^2\gamma[\frac{\cos\psi}{r\cos\phi}(c'' - c'\tan\gamma) - \frac{c'}{r\cos^2\phi}(\psi'\cos\phi\sin\psi - \\ &\quad \phi'\cos\psi\sin\phi)] \end{aligned} \tag{10}$$

Using Eqs. (4) and (10) results in

$$L = \frac{mv}{cos\sigma}[\gamma'\frac{v\cos\gamma\cos\psi}{r\cos\phi} + (\frac{\mu}{vr^2} - \frac{v}{r})\cos\gamma - \frac{T\sin\alpha\cos\sigma}{mv}] \tag{11}$$

For given values of all the state variables, Ω and σ, Eq. (11) implicitly defines the required α to follow Eq. (9), which can be solved for numerically with a Newton algorithm. Since this approach puts more direct control on the trajectory shaping by specifying r, the optimization process is more stable and much less sensitive to control variations. The histories of Ω, σ and c are parametrized as functions of θ. The corresponding trajectory is obtained by numerically integrating the equations of motion. This way, the problem becomes a parameter optimization problem and a sequential quadratic programming (SQP) algorithm has been used to solve it [15]. For instance, when the following initial and terminal conditions are used

$$r(0) = R_0 \text{ (radius of the earth)}$$

$$
\begin{aligned}
\phi(0) &= 0 \\
v(0) &= 170\ m/s\ (Mach\ 0.5) \\
\gamma(0) &= 0 \\
\psi(0) &= 0 \\
m(0) &= 133,809\ kg\ (295,000\ lbf)
\end{aligned}
\tag{12}
$$

$$
\begin{aligned}
r(t_f) &= R_o + 55\ km \\
\phi(t_f) &= 0°,\ 5°,\ 10°,\ \text{and}\ 15° \\
v(t_f) &= 7839\ m/s \\
\gamma(t_f) &= 0 \\
\psi(t_f) &= free
\end{aligned}
\tag{13}
$$

and an operational constraint

$$q \leq 95,760\ \text{N/m}^2\ (2000\ \text{psf}) \tag{14}$$

is imposed, Figure 2 depicts the ascent trajectories. They almost coincide with each other. Other features of the 3-D trajectories also closely resemble those observed in 2-D cases [4, 5, 8, 14]. The following table gives the time-of-flight and final mass for each of the trajectories. It is clear from the table that there is practically no extra penalty on the fuel consumption for 3-D trajectories as compared to the 2-D case ($\phi_f = 0°$). The reason may become evident when one inspects Figs. 3 and 4 which show the histories of bank angle $\sigma(t)$ and latitude vs. longitude, respectively. It is seen that the vehicle only uses large bank angle in a short initial period to steer it into an appropriate plane and then remains approximately in planar motion thereafter. Figure 5 confirms this feature by showing the almost constant heading angle histories of the aerospace plane, after a quick initial change that aligns the vehicle in the right direction. Therefore for the most part, an optimal 3-D trajectory is in 2-D flight.

Table 1: Time-of-flight and final mass for various final latitudes

ϕ_f(deg.)	t_f(sec.)	m_f(kg)
0	1311.2	67,112.0
5	1312.3	67,111.5
10	1312.5	67,111.1
15	1314.0	67,107.7

Thus it may be concluded that the study of 2-D flight for the aerospace plane appears to be sufficiently representative of general motion in terms of fuel consumption and characteristics of the trajectory.

3.3 Effects of Thrust Vectoring Control

The conceived configuration of the aerospace plane, which uses its forebody as part of the compressor and aftbody as part of the nozzle, probably will make thrust vectoring control (TVC) difficult to realize, and any TVC would be very limited if possible at all. However, from a trajectory analysis point of view, it would be interesting to have an assessment as how much more fuel could be saved should TVC is available. To this end, we allow a nonzero thrust angle ε to be used. The system equations are the same as Eqs. (1)–(6) with $\varepsilon \neq 0$. The study is restricted to 2-D flight. There are three control variables α, ε and Ω. Again, ε and Ω are parameterized directly and α solved using the inverse dynamic approach. The initial and terminal conditions are the 2-D versions of the conditions in Eqs. (12–13) with constraint (14) enforced.

Figure 6 shows the α and ε histories. With TVC, the final mass of the aerospace plane is 67,340 kg, comparing with 67,112 kg without TVC. The fuel saving by employing TVC is very small. This is because 75% of the optimal trajectory lies on the boundary of constraint (14). The fuel efficiency is already determined along that portion by the maximum allowable dynamic pressure (2000 psf). TVC can only improve the fuel efficiency in the short initial climbout and final zoom, which is rather limited. Consequently, the trajectory closely resembles the trajectory without TVC. Therefore one can conclude that TVC does not appear

to offer significant improvement in fuel saving in the ascent flight of an aerospace plane.

4. Analytic Treatment of Constrained Trajectories

It has been observed in the study of the optimal ascent trajectory for the aerospace plane that a dominant portion (60% – 85%) of the trajectory lies on the boundaries of the constraints (7) and (8) (Fig. 1). Because of the active constraints, it was felt that some analytic treatment to these trajectory segments may be possible, despite the nonanalytic vehicle model and nonlinearities in dynamics. Analytic solutions of the constrained trajectory as explicit functions of time, if available, would provide an efficient means to evaluate the trajectory, and often lead to a better understanding of the trajectory. In turn, tasks such as trajectory optimization, control and guidance can be significantly simplified. Reference [10], which is a product of this research, discusses this problem in a more general context. The analysis reveals that under some fairly general conditions the altitude dynamics and flight path angle dynamics constitute a natural two-time-scale system: the flight path angle dynamics is fast and the altitude dynamics slow. The asymptotic solution for the flight path angle is given as a function of the altitude from which the velocity can be expressed as an explicit function of time, regardless of the specific forms of the constraints. If the altitude can be solved in terms of the velocity from the constraint (as in the case of Eqs. (7) and (8)), both the altitude and the flight path angle have analytical expressions as functions of time. Figures 7 and 8 show the comparisons of the analytic and numerically generated altitude and flight path angle histories along a typical ascent trajectory for the aerospace plane. The accuracy is remarkable. With these closed-form solutions used for the major portion of the optimal ascent trajectory, only the relatively short initial climbout and final zoom of the trajectory need to be numerically investigated. This technique was applied in Ref. [6] successfully, demonstrating that the challenging problem of ascent trajectory optimization for the aerospace plane can be significantly simplified. The analytical solutions were also used to design a hypersonic cruising trajectory for the aerospace plane [10]. The results

strongly support the theory and the analytical solutions are in excellent agreement with the numerical results.

5. Abort Landing

As part of the investigation of the optimal trajectories for the aerospace plane, the capability of safe landing of the aerospace plane was studied. The starting point is chosen to be a typical hypersonic cruise condition. Should any propulsion system failure develop at this point, the maximum reachable distances in all directions need to be known in order to explore all abort possibilities and determine an appropriate landing site. The knowledge of this abort landing area is a particularly important information in the early stage of the test flight of such a hypersonic vehicle. The trajectory optimization problem is also known as the footprint problem [16]. The formulation of the problem is as follows:

$$\text{maximize } \phi(t_f)$$

subject to the equations of motion Eqs. (1)–(5) with $T = 0$, initial conditions

$$\begin{aligned} r(0) &= R_0 + 30.5\ km \\ \phi(0) &= 0 \\ \theta(0) &= 0 \\ v(0) &= 3351\ m/s\ (Mach\ 11) \\ \gamma(0) &= 0 \\ \psi(0) &= 0 \end{aligned} \tag{15}$$

(16)

and terminal conditions

$$\begin{aligned} r(t_f) &= R_o \\ \theta(t_f) &= \theta_f \\ v(t_f) &= 170\ m/s \end{aligned} \tag{17}$$

$$\gamma(t_f) = free$$

$$\psi(t_f) = free$$

When θ_f takes all possible values, the ground track of the point (θ_f, ϕ_f) represents the boundary of the maximum landing area (footprint). This is a 3-D trajectory optimization problem. The controls are the aerodynamic forces influenced by α and σ subject to $|\sigma| \leq 85°$. The problem is solved by directly parameterizing $\alpha(t)$ and $\sigma(t)$ and using the SQP algorithm. Figure 9 shows the footprint with the ground tracks of several trajectories. It is seen that that maximum downrange is about 2641 km and the maximum crossrange 1677 km. The minimum downrange is about -540 km (behind the starting point). The aerospace plane can glide to any landing site inside this footprint. Figure 10 illustrates some typical altitude profiles on the footprint. The oscillations in the altitude histories are characteristic of hypersonic optimal gliding trajectories [16]. The $\alpha(t)$ history for a typical trajectory is plotted in Fig. 11. We notice that the optimal α at each instant is approximately equal to the value at which the lift-to-drag ratio C_L/C_D is maximized at that Mach number. This is also consistent with what previous researchers have observed [16]. Bank angle histories for several cases are shown in Fig. 12.

6. Simultaneous Design of Trajectory and Vehicle

Because of the stringent flight path constraints and highly demanding orbital insertion conditions, fuel will be a significant part of the take-off weight of the aerospace plane. Due to the unprecedented complexity of the aerospace plane, it has been well recognized that an integrated design approach that encompasses areas of propulsion, aerodynamics, structure and flight control is a necessity for the success of the vehicle. Such an integrated approach could significantly reduce the structural weight of the vehicle and produce a far more superior design. We believe that a simultaneous design of the optimal ascent trajectory and vehicle design could also be quite beneficial in terms of further reducing the vehicle size and weight, because it has been found that there is a strong coupling between the trajectory and vehicle

structural strength requirement (e.g., the minimax dynamic pressure solution presented in Refs. [8,14]).

As a very preliminary study, we considered the trajectory optimization problem in which the control histories $\alpha(t)$ and $\Omega(t)$ (2-D case, no TVC) as well as the vehicle reference area S are to be optimized. S is chosen because it influences both aerodynamic lift, the main flight path control force, and the drag which a major portion of the fuel is spent to overcome. The initial and final conditions and constraint are the same as in Section 3.3. The optimal solution yields a reference area of 82% of the value given in the original model [12]. The final mass is 68,986 kg, comparing with 67,112 kg with the reference area fixed at the original value. It should be stressed that this result is obtained by simplistically assuming that the change of S will not influence the aerodynamic coefficients of the aerospace plane. This, of course, is not realistic. Nonetheless, the result demonstrates the significant benefits that could be achieved by combining trajectory design with the vehicle configuration design.

7. Conclusions and Future Research Topics

This report documents the major work accomplished during the period from June 1992 to October 1993. Details of some important development are not included, though, because they are available in Refs. [5–11] in the forms of archived journal papers and conference proceedings articles. Only summaries of those results are given. Other work that has not appeared in the public literature is described in greater details.

With the success of the proposed inverse dynamics approach in 2-D trajectory optimization, more complex 3-D optimal ascent was investigated. It was found that the 3-D optimal trajectory resembles the 2-D counterpart closely. In 3-D flight, the aerospace plane would initiate a tight turn after takeoff to move the trajectory into a vertical plane in which the orbit insertion point is contained. For the most part of the ascent, the trajectory remains in effect to be a 2-D trajectory. This finding indicates that the characteristics of 2-D optimal trajectories are sufficiently representative of more general cases. The study also found that

thrust vectoring control, even if available for the aerospace plane, does little to further reduce the fuel consumption in ascent. This is because the optimal ascent trajectory is tightly constrained for a dominant portion of the ascent during which the fuel consumption is mostly influenced by the allowable level of dynamic pressure. TVC only contributes to control of the relatively short initial and final segments of the trajectory.

Analytical study of constrained hypersonic trajectories was also conducted in conjunction with the findings in trajectory optimization. The work provides a general treatment to a class of constrained flight problem that include a dominant portion of the optimal ascent of the aerospace plane. By cleverly selecting the variables, the constrained dynamics are shown to be a two-time-scale system. Closed-form solutions to the constrained trajectory are obtained. These solutions were used in trajectory optimization process to significantly reduce the computation required for generating an optimal ascent trajectory.

The maximum landing area (footprint) problem accesses the safe landing capability of the aerospace plane in case the mission has to be aborted. The footprint gives the boundary of an area within which the aerospace plane can safely land by gliding from a typical hypersonic cruise altitude. The knowledge of a series of footprints corresponding to different cruise conditions would be valuable in determining the emergence landing site should any propulsion system failure of the aerospace plane develop in flight. It has been demonstrated that the trajectory optimization technique used in this research can be used to solve this problem readily.

The future research topics that seem to be logical continuation of this research are as follows

1. Simultaneous Design of Trajectory and Vehicle

   Our preliminary study has indicated that much could be gained by incorporating the vehicle design process with trajectory optimization. This multidisciplinary undertaking involves aerodynamics, propulsion, structure and flight control. Because of the scope of the challenge, initial efforts perhaps should be concentrated on proof of concept. Some

essential ingredients of each of the areas should be preserved, but simplifications are necessary for the problem to be tractable. In any event, the various models involved are most likely highly data-driven, and the size of the problem will be large. The availability of a reliable, efficient optimization algorithm that is suited for nonsmooth problem is almost imperative for any attempt to tackle this problem. Motivated by these thoughts, a recently developed continuous simulated annealing algorithm was examined, and applied for the first time to nonsmooth trajectory optimization in Ref. [9]. The algorithm demonstrated a clear superiority over some other well-known conventional algorithms in the areas such reliable convergence, efficiency and ability to find global optimum. We believe that this algorithm is a truly promising tool in any effort to study simultaneous design of ascent trajectory and vehicle.

2. Predictive Guidance Laws

From this study and previous studies, it has been observed that the optimal ascent trajectory is tightly constrained by operational and safety constraints. Thus flying along the designed path not only reduces fuel consumption, also guarantees satisfaction of mission requirements and ensures safety of the vehicle. When deviations from the nominal trajectory occur, as will inevitably in actuality, it is the job of the guidance system to provide correctional commands in real time to restore the flight path. A systematic framework for developing nonlinear feedback guidance laws is proposed in Ref. [11] which was supported in part by this grant. The approach is applicable to general nonlinear dynamics, requires no other stringent conditions on the system except the usual smoothness conditions. It is based on continuous minimization of the difference between the predicted and the nominal trajectories. The computation requirement for a typical aerospace guidance problem is well within the capability of the current onboard computers. Preliminary applications have shown its potential. A thorough evaluation of the scheme on the aerospace plane guidance problem would help identify a promising guidance law for hypersonic flight.

References

[1] Calise, A. J., Corban, J. E., and Flandro, G. A., "Trajectory Optimization and Guidance Law Development for National Aerospace Plane Applications", Final Report, NASA CR Number NAG-1-784, Dec., 1988.

[2] Corban, J. E., Calise, A. J, and Flandro, G. A., "Rapid Near-Optimal Aerospace Plane Trajectory Generation and Guidance", *Journal of Guidance, Control, and Dynamics*, Vol. 14, No. 6, November–December, 1991, pp. 1181–1190.

[3] Moerder, D. D., Pamadi, B., and Dutton, K., "Constrained Energy State Suboptimal Control Analysis of a Winged-Cone Aero-Space Plane Concept", AIAA-91-5053, *Third AIAA International Aerospace Planes Conference*, Orlando, FL, 3–5, December, 1991.

[4] Lu, P., "Trajectory Optimization and Guidance for a Hypersonic Vehicle", AIAA paper 91-5068, *Third AIAA International Aerospace Planes Conference*, Orlando, FL, Dec. 3–5, 1991.

[5] Lu, P., "An Inverse Dynamics Approach to Trajectory Optimization and Guidance for an Aerospace Plane", AIAA paper 92-4331, Proceedings of Guidance, Navigation and Control Conference, Hilton Head, SC, August 10–12, 1992.

[6] Lu, P., and J. Samsundar, "Closed-Form Solution of Constrained Trajectories: Application in Optimal Ascent of Aerospace Planes",*Fourth AIAA International Aerospace Planes Conference*, Orlando, FL, Dec. 2–4, 1992.

[7] Samsundar, J., "An Investigation of Optimal Trajectories for an Aerospace Plane", M. S. Thesis, Iowa State University, May, 1993.

[8] Lu, P., "Inverse Dynamics Approach to Trajectory Optimization for an Aerospace Plane", *Journal of Guidance, Control, and Dynamics*, Vol. 16, No. 4, 1993, pp. 726–732.

[9] Lu, P., and Khan, M. A., "Nonsmooth Trajectory Optimization: An Approach Using Continuous Simulated Annealing", *Proceedings of Atmospheric Flight Mechanics Conference*, Monterey, CA, August9–11, 1993. Also to appear in *Journal of Guidance, Control, and Dynamics*, 1994

[10] Lu, P., "Analytical Solutions to Constrained Hypersonic Flight Trajectories", *Journal of Guidance, Control, and Dynamics*, Vol. 16, No. 5, 1993, pp. 956–960.

[11] Lu, P. and Khan, M. A., "Predictive Guidance Laws", submitted to *Guidance, Navigation, and Control Conference*, Scottsdale, AZ, 1994.

[12] Shaughnessy, J. D., Pinckey, S. Z., McMinn J. D., Cruz, C. I., and Kelley M-L., "Hypersonic Vehicle Simulation Model: Winged-Cone Configuration", NASA TM 102610, November 1990.

[13] Powell, R. W., Shaughnessy, J. D., Cruz, C. I., and Naftel, J. C., "Ascent Performance of an Air-Breathing Horizonal-Takoff Launch Vehicle", *Journal of Guidance, Control, and Dynamics*, Vol. 14, No. 4, 1991, pp. 834–839.

[14] Lu, P., "Trajectory Optimization for the National AeroSpace Plane", Final Report, NASA Grant NAG 1-1255, June, 1992.

[15] Pouliot, M. R., "CONOPT2: A Rapidly Convergent Constrained Trajectory Optimization Program for TRAJEX", Report N0. GDC-SP-82-008, General Dynamics, Convair Division, San Diego, CA, 1982.

[16] Vinh, N. X., *Optimal Trajectories in Atmospheric Flight*, Elsevier Scientific Publishing Company, Amsterdam, The Netherlands, 1981

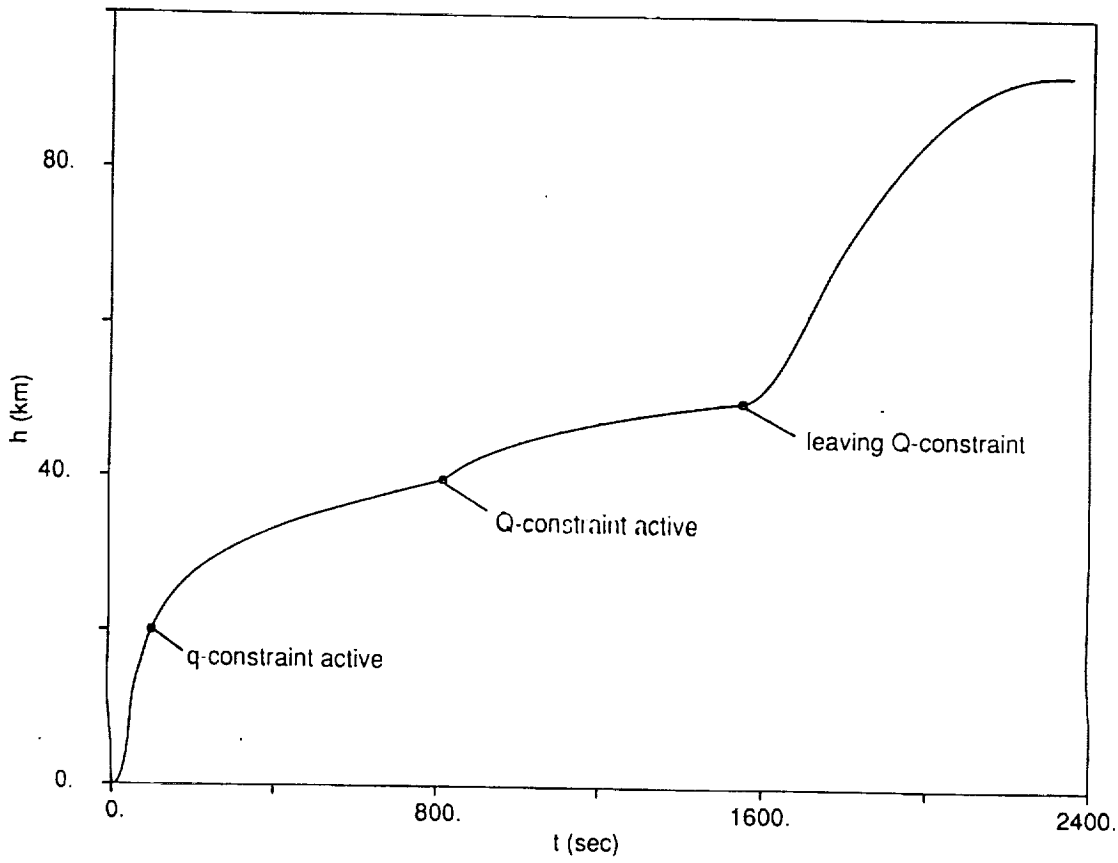

Figure 1: Typical 2-D optimal ascent trajectory

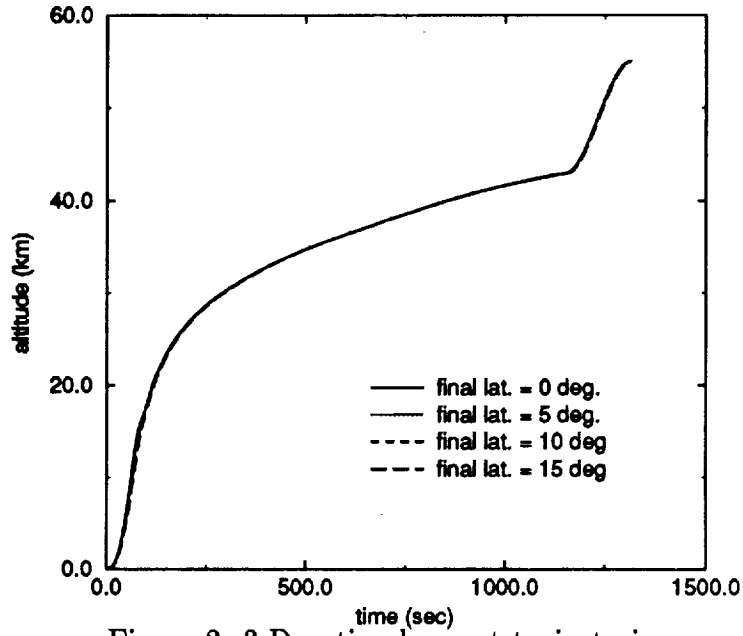

Figure 2: 3-D optimal ascent trajectories

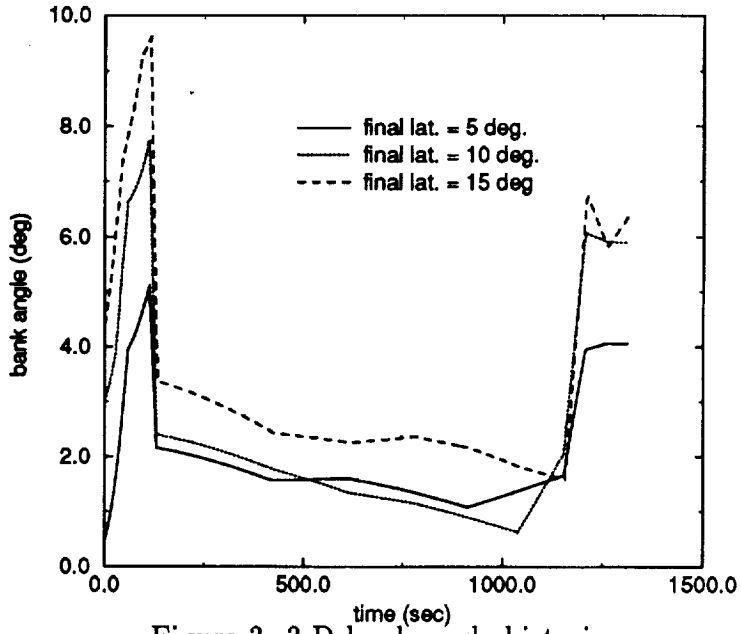

Figure 3: 3-D bank angle histories

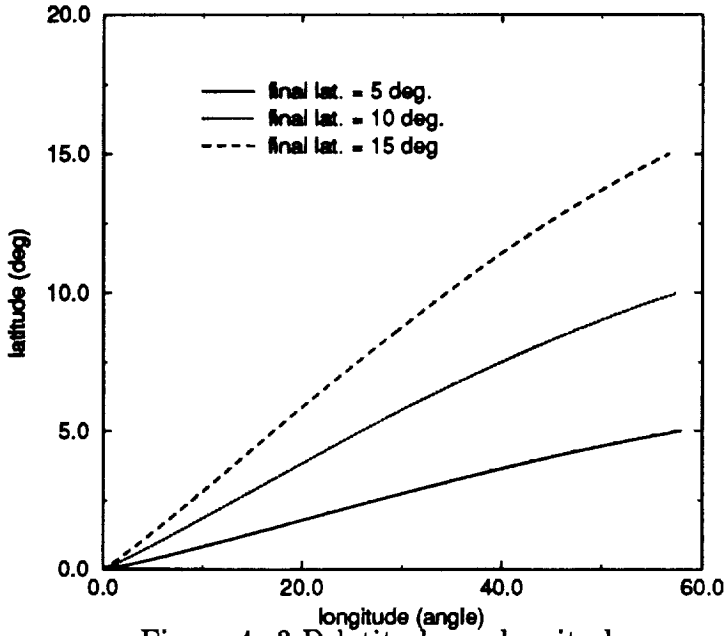

Figure 4: 3-D latitude vs. longitude

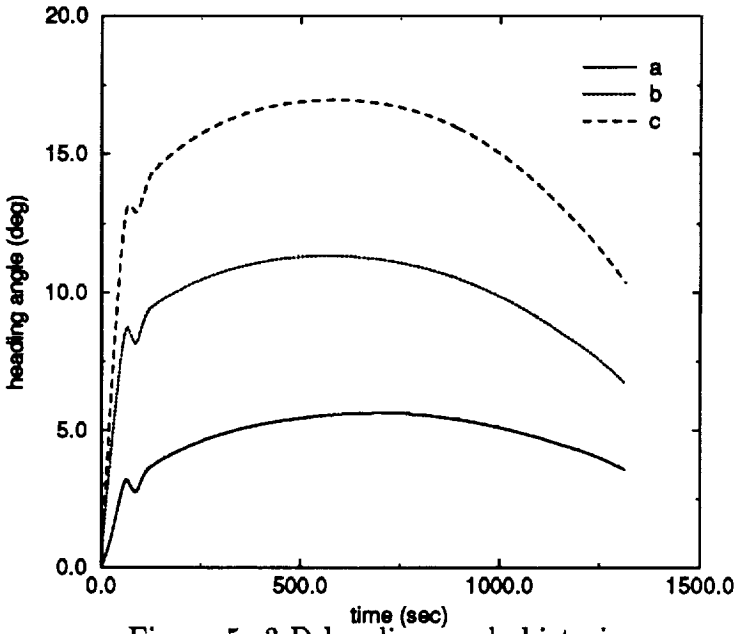

Figure 5: 3-D heading angle histories

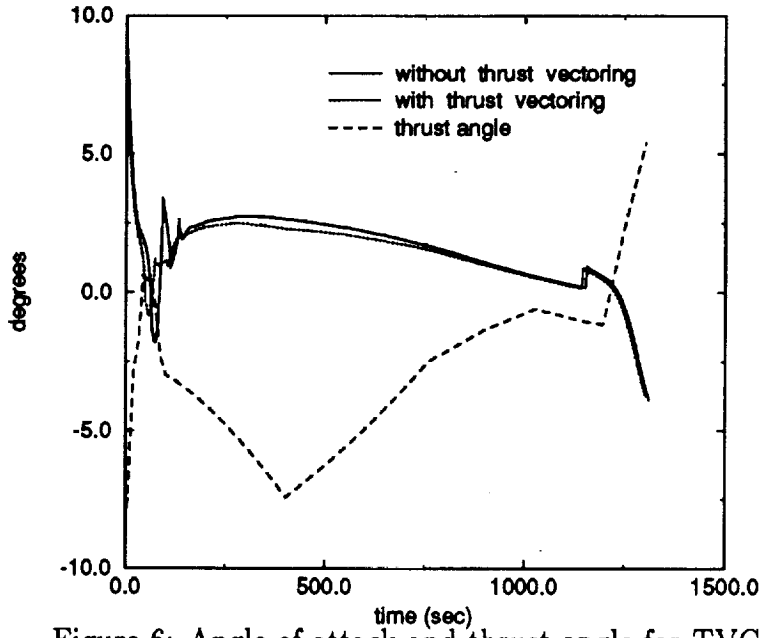

Figure 6: Angle of attack and thrust angle for TVC

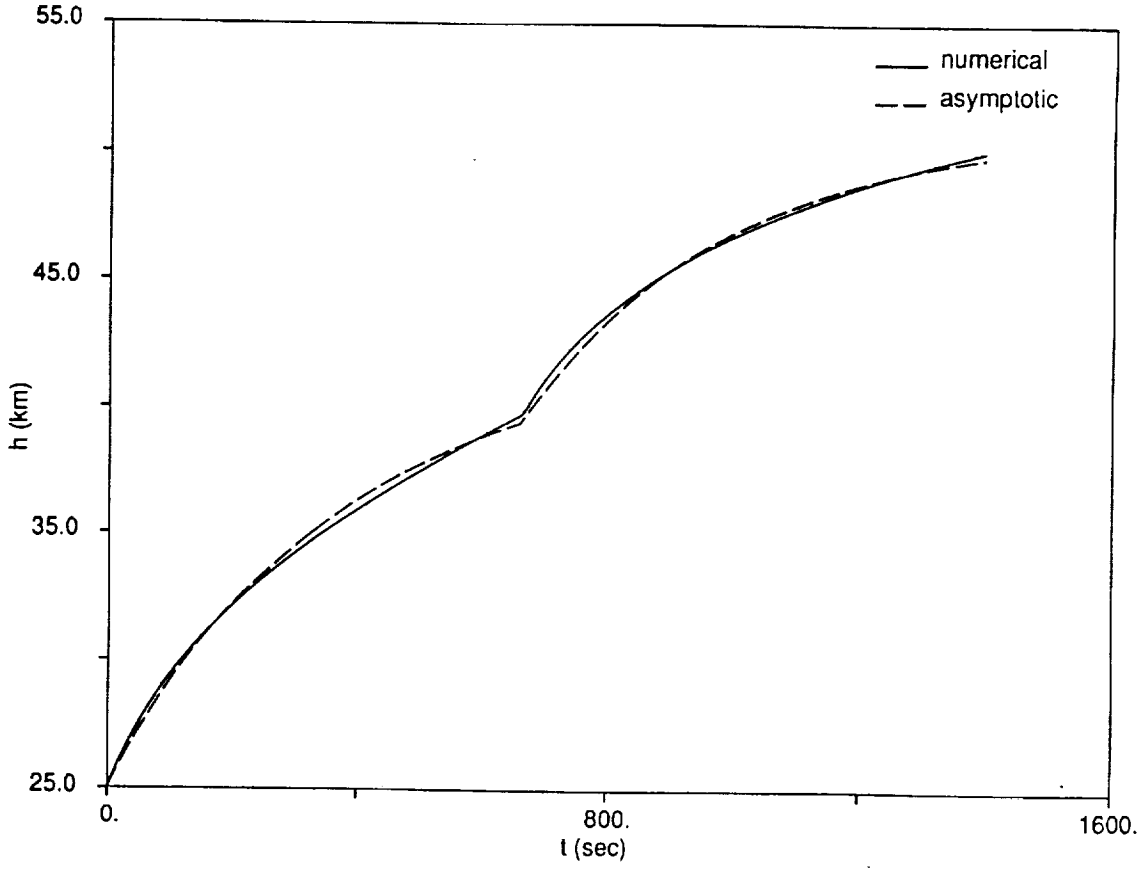

Figure 7: Comparison of analytical and numerical altitude histories

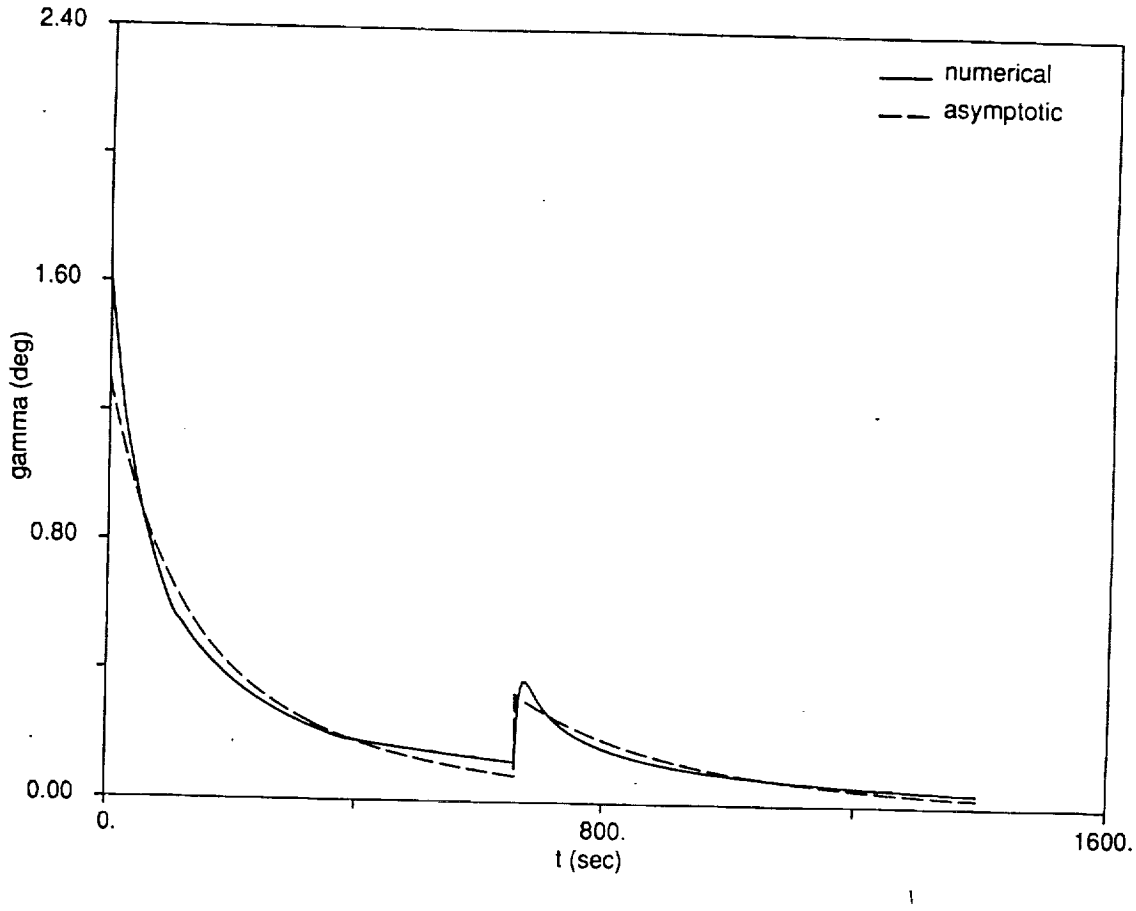

Figure 8: Comparison of analytical and numerical flight path angle histories

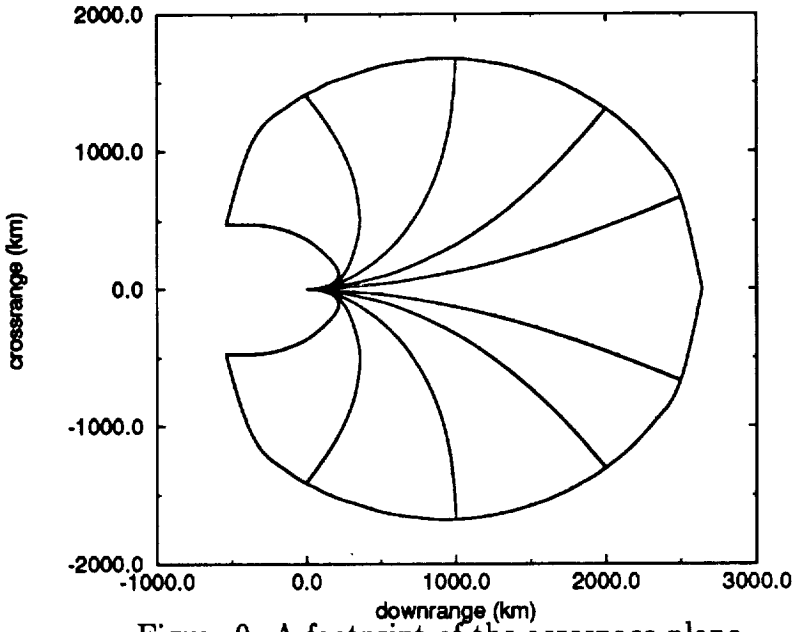

Figure 9: A footprint of the aerospace plane

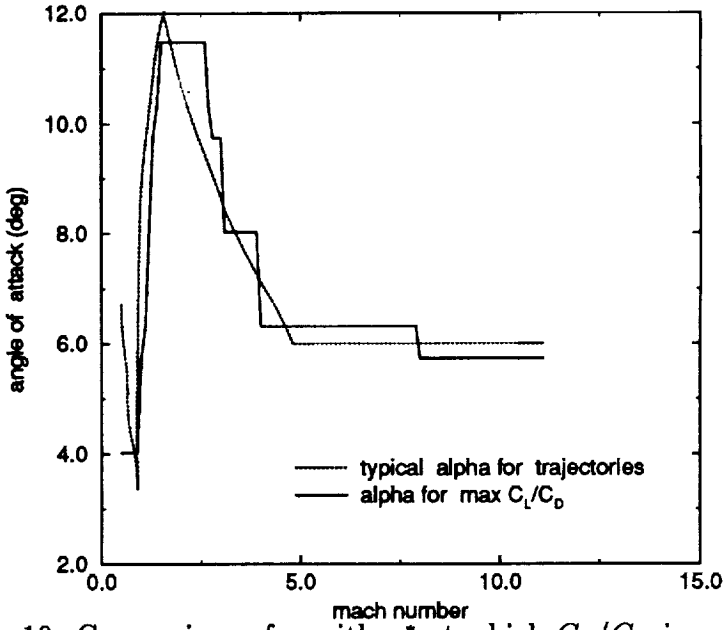

Figure 10: Comparison of α with α^* at which C_L/C_D is maximized

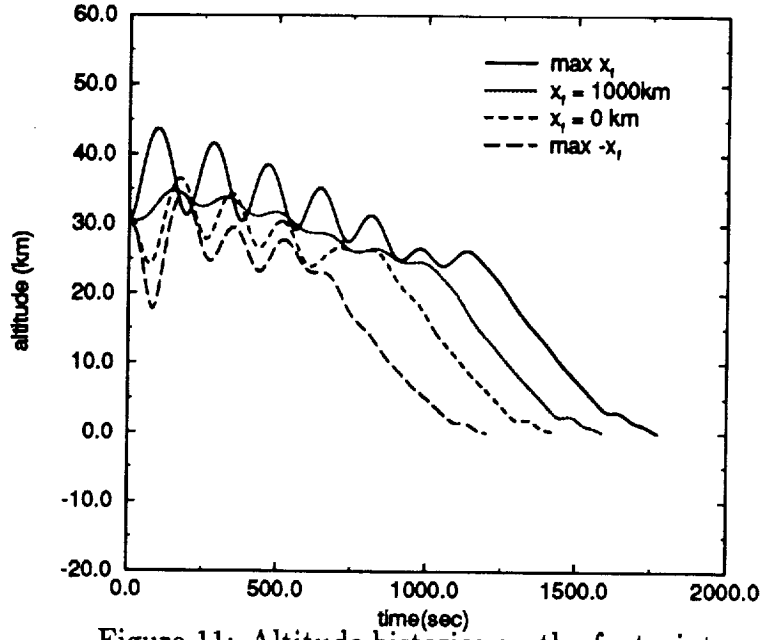

Figure 11: Altitude histories on the footprint

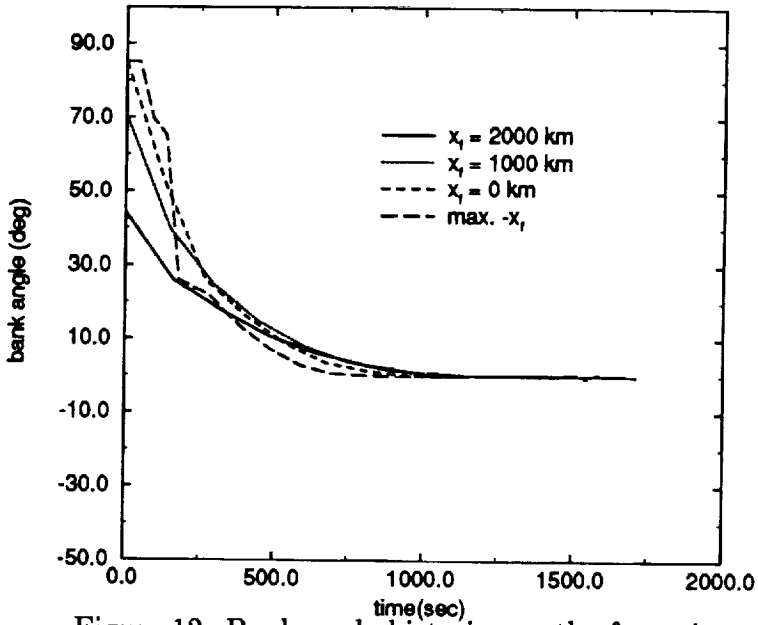

Figure 12: Bank angle histories on the footprint